Published in final edited form as:
Acta Neuropathol. 2011 February ; 121(2): 287–289. doi:10.1007/s00401-010-0776-9.

Parallel fiber counts and parallel fiber integrated density are similar in essential tremor cases and controls

Sheng-Han Kuo,
Department of Neurology, College of Physicians and Surgeons, Columbia University, New York, NY, USA

Phyllis L. Faust,
Department of Pathology and Cell Biology, College of Physicians and Surgeons, Columbia University, New York, NY, USA

John-Paul G. Vonsattel,
Department of Pathology and Cell Biology, College of Physicians and Surgeons, Columbia University, New York, NY, USA

Taub Institute for Research on Alzheimer's Disease and the Aging Brain, College of Physicians and Surgeons, Columbia University, New York, NY, USA

Karen Ma, and
GH Sergievsky Center, College of Physicians and Surgeons, Columbia University, New York NY, USA

Elan D. Louis
Department of Neurology, College of Physicians and Surgeons, Columbia University, New York, NY, USA

Taub Institute for Research on Alzheimer's Disease and the Aging Brain, College of Physicians and Surgeons, Columbia University, New York, NY, USA

GH Sergievsky Center, College of Physicians and Surgeons, Columbia University, New York NY, USA

Department of Epidemiology, Mailman School of Public Health, Columbia University, New York, NY, USA

Unit 198, Neurological Institute, 710 West 168th Street, New York, NY 10032, USA

Elan D. Louis: EDL2@columbia.edu

Essential tremor (ET) is one of the most common neurological diseases, yet the number of published postmortem examinations is limited, and the range of pathological changes associated with this disease has yet to be fully catalogued. Aside from Purkinje cell (PC) loss and increased numbers of PC axonal swellings (torpedoes) in ET, hypertrophic changes

Correspondence to: Elan D. Louis, EDL2@columbia.edu.

Conflict of interest The authors report no conflicts of interest.

in basket cell axonal plexuses have recently been identified [6], thus triggering the question whether other compensatory architectonic changes occur in the molecular or PC layers in this disease. To our knowledge, parallel fibers (PFs) have not been systematically quantified in ET cases versus matched controls.

Postmortem cerebellar tissue was obtained from 20 ET cases without Lewy bodies and 19 non-diseased age-matched controls at the Essential Tremor Centralized Brain Repository (ETCBR), Columbia University, New York. All brains had complete neuropathological assessment [4]. Ascertainment of ET cases and controls and diagnosis of ET cases has been described [4].

A standard 3 × 20 × 25 mm parasagittal neocerebellar cortex tissue block was harvested from each brain. Paraffin sections (7 μm thick) were stained with a modified Bielschowsky silver method. Each brain had standardized measurement of brain weight (grams), postmortem interval (PMI), neurofibrillary pathology staging of Braak et al., and Consortium to Establish a Registry for AD (CERAD) rating [1, 7]. PCs and torpedoes were quantified as described [4].

Digital images of the Bielschowsky neocerebellum preparations were obtained from two selected regions in each brain using a Zeiss Axioplan 2 microscope fit with an Axiocam HR digital camera (20× objective lens). The two selected regions, both from the most centrally located folium in the section, were a distal gyrus and a distal sulcus. Each selected region was 200 μm in width and situated just above the PC layer (Fig. 1a, b). The height of each region, 160 μm, allowed for quantification of most of the stained PFs in the molecular layer. Each PF was manually traced using the tracing tool in Adobe Photoshop Element 6.0 (Fig. 1c). PFs were identified as the fibers oriented parallel to the PC layer. Fibers oriented >45 degrees to the PC layer were excluded, as were PC dendrites and baskets. Images of the PF tracings were inverted and imported into Image J (NIH), where integrated density was calculated, as described [4]. We averaged five randomly-selected background values (high in the molecular layer, with no visible PFs) and divided the integrated density by the average background value to obtain a PF integrated density (PFID) for each of the two regions. As the PFIDs in the two regions were highly correlated (Pearson's $r = 0.66$, $p < 0.001$), we reported the average of those two PFIDs. Also, a PF count (PFC) was obtained by drawing an index line at the center of each image, and counting the number of PFs that crossed that line (Fig. 1b). The PFC we report was the average of those two PF counts, and was highly correlated with the PFID (Pearson's $r = 0.59$, $p < 0.001$).

Cases and controls were similar in age, gender, brain weight and PMI but, as expected, cases had more torpedoes and lower PC counts than controls (Table 1). Braak AD scores were higher in ET cases than controls, although CERAD scores did not differ (Table 1). The PFID and PFC did not correlate with age, brain weight, PMI, torpedoes, Braak AD stage, or CERAD score. The PFC correlated weakly and inversely with PC counts (Pearson's $r = -0.34$, $p = 0.04$) and was lower in women than men ($p = 0.005$). Cases and controls were similar with respect to both the PFID and the PFC (Table 1). We assessed the role of several possible confounding factors. In a linear regression analysis that adjusted for gender, Braak AD stage and PC counts, PFC (outcome variable) did not differ by case–control status (beta

= 1.54, $p = 0.37$). In a linear regression analysis that adjusted for Braak AD stage, PFID did not differ by case–control status (beta = 2899.4, $p = 0.80$).

One limitation of this study is that the Bielschowsky method may not stain all PFs, yet we have no reason to suspect that this would be differential between cases and controls. Also, some of the fibers oriented parallel to the PC layer may have been basket cell processes rather than PCs. Finally, use of other staining methods (e.g., neurofilament antibody) could allow for additional case–control comparisons.

Our analyses did not indicate a reduction in PFs in ET. Studies in PC and granule cell death demonstrate that different pathways are involved. PC death involves an autophagic pathway whereas granule cell death is predominantly apoptotic [2, 3]. In sporadic Creutzfeldt-Jakob disease, another cerebellar degenerative disease, granule cell death is marked yet PCs are relatively preserved [5], providing an example of the dissociation between PC and granule cell death. Our findings suggest that in ET, cerebellar degeneration is specific to PCs whereas PFs may be preserved.

Acknowledgments

R01 NS42859 from the National Institutes of Health (Bethesda, MD).

References

1. Braak H, Alafuzoff I, Arzberger T, Kretzschmar H, Del Tredici K. Staging of Alzheimer disease-associated neurofibrillary pathology using paraffin sections and immunocytochemistry. Acta Neuropathol. 2006; 112:389–404. [PubMed: 16906426]
2. Contestabile A. Cerebellar granule cells as a model to study mechanisms of neuronal apoptosis or survival in vivo and in vitro. Cerebellum. 2002; 1:41–55. [PubMed: 12879973]
3. Dusart I, Guenet JL, Sotelo C. Purkinje cell death: differences between developmental cell death and neurodegenerative death in mutant mice. Cerebellum. 2006; 5:163–173. [PubMed: 16818391]
4. Erickson-Davis CR, Faust PL, Vonsattel JGV, Gupta S, Honig LS, Louis ED. “Hairy baskets” associated with degenerative Purkinje cell changes in essential tremor. J Neuropathol Exp Neurol. 2010; 69:262–271. [PubMed: 20142764]
5. Ferrer I. Synaptic pathology and cell death in the cerebellum in Creutzfeldt-Jakob disease. Cerebellum. 2002; 1:213–222. [PubMed: 12879983]
6. Louis ED. Essential tremor: evolving clinicopathological concepts in an era of intensive postmortem inquiry. Lancet Neurol. 2010; 9:613–622. [PubMed: 20451458]
7. Mirra SS. The CERAD neuropathology protocol and consensus recommendations for the postmortem diagnosis of Alzheimer’s disease: a commentary. Neurobiol Aging. 1997; 18:S91–S94. [PubMed: 9330994]

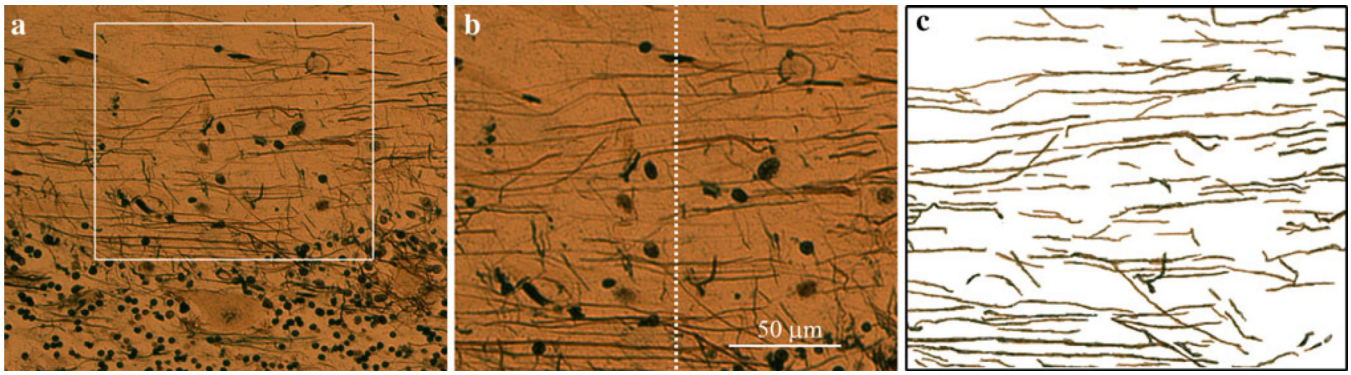

Fig. 1.

a Cerebellar cortical section (200× magnification, modified Bielschowsky silver method), showing PFs. A selected region was 200 μm in width and situated just above the PC layer. PFs within that region were analyzed. **b** A PFC was obtained by drawing an index line at the center of each image, and counting the number of PFs that crossed that line. **c** PFs were traced as described and PFID was obtained

Table 1

Clinical and pathological features of ET cases and controls

	ET	Controls
N	20	19
Age (years)	83.0 ± 8.3	82.5 ± 7.4
Female gender	65%	47.4%
Brain weight (g)	1,209 ± 106	1,232 ± 112
Postmortem interval (h)	4.6 ± 3.4	7.1 ± 7.8
Braak AD stage (median, range) *	2.0, 0–4	1.0, 0–4
[a]CERAD plaque score (median, range)	0, 0–3	0, 0–1
[b]PC count *	31.8 ± 6.4	46.0 ± 12.6
[b]Axonal torpedoes *	13.3 ± 13.9	2.7 ± 2.9
Parallel fiber integrated density	23798.2 ± 16789.7	33515.1 ± 36261.0
Parallel fiber count	11.3 ± 4.2	10.3 ± 4.1

Mean ± standard deviation and frequency (%) are reported unless otherwise specified

* $p < 0.01$, cases versus controls. Student's *t* test was used for comparisons of means, Mann–Whitney test was used for comparison of medians, and χ^2 tests were used for comparison of proportions

[a] CERAD plaque scores were converted from letters to numbers: 0, absent; 1, sparse; 2, moderate; and 3, severe

[b] In each brain, torpedoes in the entire 3 × 20 × 25 mm section were counted, and PCs in five 100× fields were counted and averaged